

# X-ray and optical pulse interactions in GaAs

Cite as: J. Appl. Phys. **122**, 243101 (2017); <https://doi.org/10.1063/1.5005812>

Submitted: 19 September 2017 . Accepted: 01 December 2017 . Published Online: 22 December 2017

Stephen M. Durbin , Tharun Nagulu, and Anthony D. DiChiara



View Online



Export Citation



CrossMark

## ARTICLES YOU MAY BE INTERESTED IN

[Perspective: Terahertz science and technology](#)

Journal of Applied Physics **122**, 230901 (2017); <https://doi.org/10.1063/1.5007683>

[234nm and 246nm AlN-Delta-GaN quantum well deep ultraviolet light-emitting diodes](#)

Applied Physics Letters **112**, 011101 (2018); <https://doi.org/10.1063/1.5007835>

[Bidirectional reconfiguration and thermal tuning of microcantilever metamaterial device operating from 77K to 400K](#)

Applied Physics Letters **111**, 261101 (2017); <https://doi.org/10.1063/1.5006836>

## Ultra High Performance SDD Detectors



See all our XRF Solutions

# X-ray and optical pulse interactions in GaAs

Stephen M. Durbin,<sup>1,a)</sup> Tharun Nagulu,<sup>1</sup> and Anthony D. DiChiara<sup>2</sup>

<sup>1</sup>Department of Physics and Astronomy, Purdue University, West Lafayette, Indiana 47906, USA

<sup>2</sup>Advanced Photon Source, Argonne National Laboratory, Argonne, Illinois 60439, USA

(Received 19 September 2017; accepted 1 December 2017; published online 22 December 2017)

Absorption of hard x-rays in GaAs creates excitations that can dramatically alter the propagation of optical laser pulses with photon energies near the bandgap. Measurements of optical transmission through a thin crystalline wafer of GaAs after absorption of an intense x-ray synchrotron pulse demonstrate how x-ray induced optical transparency depends on the recombination of excited conduction band electrons and valence band holes via Auger, spontaneous emission, and especially stimulated emission processes. The x-ray induced band fluorescence spectrum also reveals amplified spontaneous emission at the high x-ray fluences used, confirming the importance of stimulated emission. For laser pulses with sufficiently high fluence, the interaction of optically excited electrons with x-ray excited electrons can quench the enhanced laser transmission. *Published by AIP Publishing.* <https://doi.org/10.1063/1.5005812>

## I. INTRODUCTION

Understanding x-ray induced optical properties is becoming increasingly important with the rapid development of x-ray free electron laser (XFEL) sources and with continuous progress towards higher brightness x-ray synchrotrons, both of which allow for higher pulse energies to be delivered to smaller sample volumes. X-ray induced optical reflectivity and transmission with semiconductors have been employed to characterize the femtosecond duration of XFEL pulses.<sup>1–4</sup> X-ray induced perturbations to optical polarization have been suggested as a possible time-resolved detection mechanism with a picosecond resolution.<sup>5</sup> X-ray induced optical transparency in GaAs has already been demonstrated with  $\sim 80$  ps x-ray pulses at a synchrotron source.<sup>6</sup> There are also efforts to use the x-ray pulses themselves to generate optical excitations using non-linear four-wave mixing schemes at XFELs.<sup>7</sup>

The separation of valence and conduction band states by a gap plays a key role in a semiconductor's interactions with hard x-ray photons as well as with optical photons. Absorption of hard x-rays by deep core levels leads to both photoelectrons and subsequent Auger electrons that lose their kinetic energy by promoting valence electrons into the conduction band, just as an optical photon is absorbed by promoting a valence electron into the conduction band. These electronic excitations can then interact with the x-ray and laser pulses. For example, excitations created by the leading edge of a high fluence optical pulse can reduce absorption of the remainder of the pulse, leading to non-linear transmission effects. An intense x-ray pulse can create high densities of electrons and holes that empty the top of the valence band and fill the bottom of the conduction band such that transmission of subsequent optical photons is controlled by Pauli blocking and results in x-ray induced optical transparency.<sup>6</sup> While these x-ray excited electrons and holes will typically recombine to generate optical fluorescence, for the highest excitation densities, an incident

laser pulse could induce stimulated emission. That is, the semiconductor could serve as a gain medium where an x-ray pulse increases the laser pulse intensity, creating an x-ray pumped semiconductor optical amplifier. Excited electrons and holes thus mediate the interaction between x-ray and laser pulses, making electron-hole dynamics critical for determining the temporal characteristics of coupled x-ray and optical pulse interactions in semiconductors.

## II. PICOSECOND X-RAY AND OPTICAL PROBING OF GALLIUM ARSENIDE

We report here on measurements of x-ray and optical laser pulse interactions using a simple transmission geometry (Fig. 1). A commercial wafer of semi-insulating GaAs with standard optically polished surfaces was thinned on one side by acid etching to a thickness of  $\sim 40$   $\mu\text{m}$ , leaving a somewhat roughened surface on the backside. This specimen was positioned at a  $45^\circ$  angle midway between a horizontal x-ray synchrotron beam and a vertical laser beam incident from above. The x-ray and laser beams were carefully aligned to intersect, and the GaAs sample could be positioned to set the intersection point at various depths within the sample.

The x-ray source was a synchrotron beamline (the Advanced Photon Source sector 14) that delivered isolated x-ray pulses ( $\sim 80$  ps FWHM) at the rate of 41 Hz.<sup>8</sup> The energy per pulse was  $\sim 10$   $\mu\text{J}$ , an orders of magnitude enhancement achieved by taking the unmonochromated output of dual undulators, and the x-rays were focused with mirrors to a rectangular spot size on the sample of  $\sim 25 \times 50$   $\mu\text{m}$ . The x-ray intensity could be reduced by a factor of  $\sim 7$  by the insertion of a Ti filter. The x-ray energy was set to 12 keV, slightly above the *K* absorption edges of both Ga (10.36 keV) and As (11.86 keV), for an absorption length of  $\sim 12$   $\mu\text{m}$ . Even though the x-ray path through the sample is more than five absorption lengths (exponential reduction factor = 0.003), we will see that x-ray absorption generates significant conduction electron densities across the entire sample thickness. We also measured the optical fluorescence generated by x-ray

<sup>a)</sup>durbin@purdue.edu

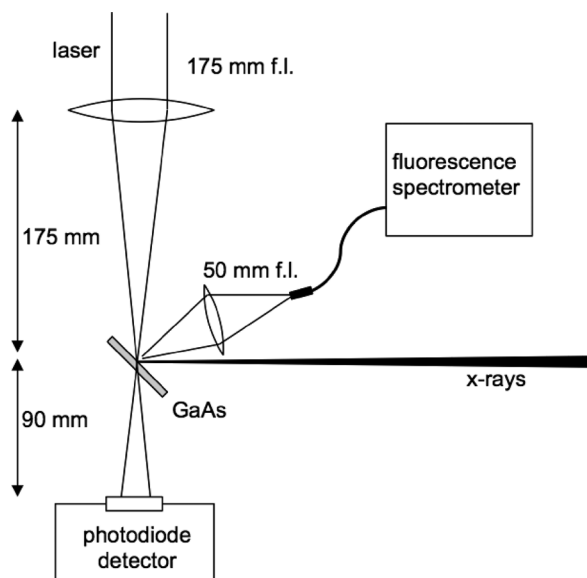


FIG. 1. Experimental layout. The thin GaAs specimen is oriented at 45 degrees to the horizontal x-ray and vertical laser beams. A 175 mm focal length lens focuses the laser light onto the sample. The transmitted light is detected 90 mm below by a Si photodiode detector. A 50 mm focal length lens collects optical fluorescence from the top surface of the GaAs specimen, which is focused onto an optical fiber and analyzed using a spectrometer.

absorption, collected from the top sample surface by a lens, and analyzed using an optical spectrometer. That is, we measured the spectrum of light emitted when electrons excited into the conduction band after x-ray absorption recombine with valence holes, which spans a region around the bandgap energy broadened by the occupied densities of states of electrons and holes.

The laser pulses (1 ps FWHM) were set to a wavelength of  $\sim 880$  nm, which corresponds to 1.41 eV per photon, just below the nominal 1.42 eV bandgap of GaAs but well within the absorbing Urbach tail region and hence above the effective bandgap. The optical absorption length (without x-rays present) was about  $\mu_L^{-1} \sim 6 \mu\text{m}$ . The pulses were focused by a lens to  $\sim 20 \times 25 \mu\text{m}$  on the sample, somewhat smaller than the x-ray spot. Transmission through the sample for a laser pulse energy of 10 nJ (a fluence of  $20 \text{ J/m}^2$ ) could not be detected above the noise level of the Si photodiode detector (in the absence of x-rays), but enhanced transmission was seen for pulse energies of 40 nJ and above. The laser pulses are synchronized to the x-ray pulses to allow control of their time delay, with a measured jitter of  $\sim 10$  ps.

### III. X-RAY INDUCED OPTICAL TRANSPARENCY AND STIMULATED EMISSION

Figure 2(b) shows the transmitted laser signal as a function of delay time between x-ray and laser pulses for nominal intersection  $30 \mu\text{m}$  below the surface. The laser pulse energy is 40 nJ (fluence  $80 \text{ J/m}^2$ ), which exhibits a barely detectable level of transmission without x-rays, but after x-ray absorption, the peak laser transmission increases to roughly 10% of the incident light. A very different lineshape is seen from a second dataset, taken after a factor of 7 reduction in x-rays, demonstrating a non-linear dependence on the amount of

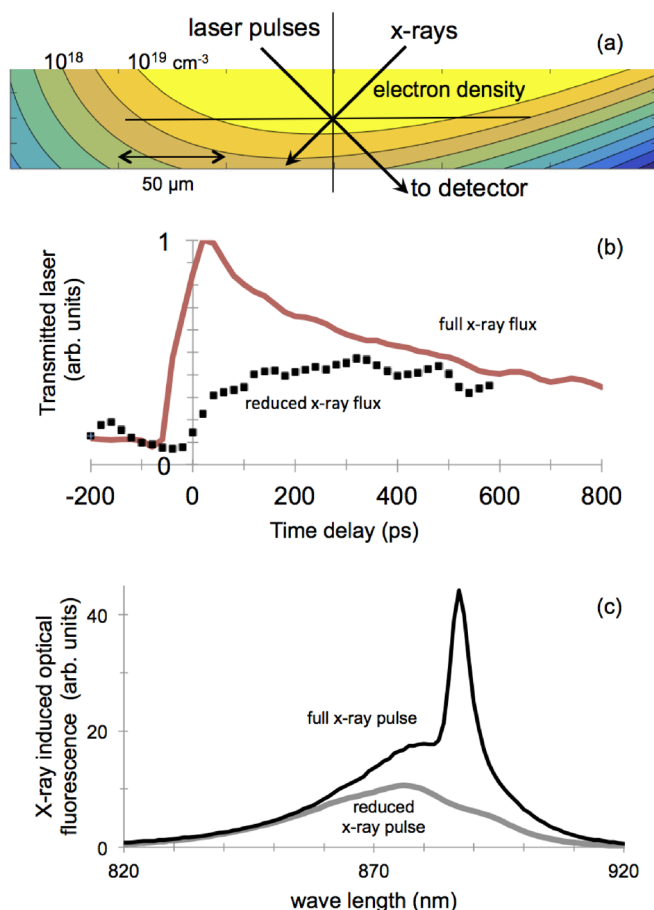


FIG. 2. X-ray induced optical transparency. (a) Experimental configuration showing perpendicular x-ray and laser beams intersecting inside a  $48 \mu\text{m}$  thick wafer of GaAs. Contour lines denote the calculated conduction electron density ( $\text{cm}^{-3}$ ) at a 100 ps time delay after arrival of an x-ray pulse, with a laser/x-ray intersection point at a depth of  $30 \mu\text{m}$ . (b) Red curve is the laser transmission (arbitrary units) through the GaAs wafer versus x-ray pulse/laser pulse time delay, for a laser fluence of  $80 \text{ J/m}^2$ , an x-ray fluence of  $8 \text{ kJ/m}^2$ , and an intersection depth of  $30 \mu\text{m}$ ; data points are for x-rays reduced by a factor of  $\sim 7$ . (c) X-ray induced band fluorescence from the top surface. The upper curve is the optical spectrum obtained from x-ray excitation with  $10 \mu\text{J}$  pulses, a radiant exposure of  $\sim 8 \text{ kJ/m}^2$  per pulse; the lower curve is the scaled output from x-ray pulse energies reduced by a factor of  $\sim 7$ . The prominent line at 885 nm indicates amplified spontaneous emission.

x-ray absorption. The time dependence of the x-ray induced optical transparency must depend on the concentration of electrons excited into the conduction band, whose dynamics is governed by recombination with holes, Auger processes, etc. To evaluate the likelihood of laser-induced stimulated emission contributing to the recombination dynamics, we measured the x-ray induced optical fluorescence. Figure 2(c) shows the data obtained for the full x-ray intensity and after reducing the x-ray beam by a factor of 7 using a Ti filter.

The reduced pulse energy spectrum displays a typical broad fluorescence spectrum corresponding to the recombination of excited electrons and holes across the bandgap. For the full x-ray pulse energy, however, a well-defined peak appears near 885 nm ( $\sim 1.41$  eV) on top of the broad spectrum, unmistakable evidence of selective optical amplification. Since there is no laser pulse to stimulate the emission, this is instead amplified spontaneous emission (ASE). This phenomenon can occur in any direction in the sample, but

previous studies<sup>9</sup> of AlGaAs heterostructures found that the threshold electron density for modes propagating parallel to the surface is lower than that in the perpendicular direction, i.e.,  $\sim 10^{18}$  vs.  $10^{20} \text{ cm}^{-3}$ , due to shorter gain lengths in the surface normal direction. Hence, surface ASE indicates that it must also be present in the lateral direction, and therefore, we will include stimulated emission in our modeling below.

Figure 2(a) shows an example of the calculated x-ray induced conduction electron density, in this case for a 100 ps delay and 30  $\mu\text{m}$  intersection point. The conduction electron density is obtained by numerically solving the differential equation combining the creation of electron-hole pairs from absorbed x-rays with their decay due to spontaneous emission and Auger processes

$$\frac{dn(\vec{r}, t)}{dt} = A(\vec{r}, t) - Bn^2(\vec{r}, t) - Cn^3(\vec{r}, t), \quad (1)$$

where

$$\begin{aligned} A(\vec{r}, t) = & \left( \frac{E_P}{E_{e-h}} \right) \mu_X I_{xray}(\vec{r}, t) = \left( \frac{E_P}{E_{e-h}} \right) \mu_X e^{-\mu_X l} \\ & \times \left\{ \frac{N}{2\pi\sigma_x\sigma_y} \exp \left[ -\frac{1}{2} \left[ \left( \frac{\Delta_x}{\sigma_x} \right)^2 + \left( \frac{\Delta_y}{\sigma_y} \right)^2 \right] \right] \right\} \\ & \times \frac{1}{\sqrt{2\pi}\sigma_\tau} e^{-\frac{1}{2} \left[ \frac{t}{\sigma_\tau} \right]^2}. \end{aligned} \quad (2)$$

We assume published coefficients<sup>10</sup> for recombination from spontaneous emission,  $B = 1.7 \times 10^{-10} \text{ cm}^3/\text{s}$ , and Auger recombination,  $C = 7 \times 10^{-30} \text{ cm}^6/\text{s}$ . The creation of excited electrons  $A(\vec{r}, t)$  is the rate at which x-ray energy is absorbed and converted into electron-hole pairs. The intensity of x-rays at any point  $I_{xray}(\vec{r}, t)$  depends on the relative distance  $\Delta_x/\sigma_x$  and  $\Delta_y/\sigma_y$  from the central ray of the x-ray beam, where  $\sigma_x$  and  $\sigma_y$  are the Gaussian x-ray beam widths in the  $x$  and  $y$  directions. The time profile of the x-ray beam is also Gaussian, with  $\sigma_\tau = 35 \text{ ps}$ . The x-ray absorption length is  $\mu_x^{-1} = 12 \mu\text{m}$ ,  $l$  is the length along the x-ray beam, and the total number of 12 keV x-rays per pulse is  $N = 10^{10}$ . The average number of electron-hole pairs created by the absorption of one x-ray photon is represented by  $E_X/E_{e-h}$ , with  $E_X = 12 \text{ keV}$  and  $E_{e-h}$  estimated to be 10 eV.<sup>11</sup>

Optical transmission calculations first require determining the conduction band electron density for each position and time sampled by a laser pulse. We then assign an absorption coefficient for the laser beam at each volume element along the laser beam path, taking into account the laser's Gaussian spatial profile and sequentially calculating the throughput along a given path parallel to the laser using  $I(\vec{r}_{k+1}) = \alpha(\vec{r}_k)I(\vec{r}_k)$ , where  $\alpha(\vec{r}_k) = e^{-\mu_k \Delta r}$  is the local absorption factor across the displacement  $\Delta r = |\vec{r}_{k+1} - \vec{r}_k|$  (typically set to 1  $\mu\text{m}$ ).

The absorption of a laser photon of energy  $E_P$  depends on the joint probability of a filled valence band state and an empty conduction band state separated by  $E_P$ . This entails the Fermi-Dirac function  $f_{FD}$  and Fermi energies  $E_{FC}$  and  $E_{FV}$  for the conduction and valence bands, which depend on the electron density  $n(\vec{r}, t)$  determined from Eq. (1). For an ideal semiconductor with parabolic bands (i.e., density of states

$D_{cond} \sim (E - E_c)^{1/2}$ ), standard approximations can be used to determine the Fermi energies for a given  $n(\vec{r}, t)$ .<sup>12,13</sup> The absorption factor is given by<sup>14,15</sup>

$$\alpha(n) = C \int \mathcal{D}_{cond}(E) [1 - f_{FD}(E, E_{FC})] \times \mathcal{D}_{val}(E - E_P) f_{FD}(E - E_P, E_{FV}) dE. \quad (3)$$

The limits of integration are from  $E_c$  (the bottom of the conduction band) to  $E_c + E_P - E_g$ , where the photon energy  $E_P$  is greater than the bandgap  $E_g$ . The constant  $C$  is adjusted to yield the actual absorption factor for the chosen laser wavelength in the absence of x-ray excitation. Calculations based on the Nilsson approximation for the Fermi energy plus textbook parameters for the parabolic approximation to the densities of states yielded the curve (square symbols) in Fig. 3 labeled “ideal bands.” The corresponding fit to the data (acquired with an incident laser fluence of 80 J/m<sup>2</sup>) for this simple model (Fig. 3 top, “ideal bands” curve), however, needs improvement.

The ideal band absorption curve closely follows the shape of an error function vs. the log of the electron density. To simplify modeling (and improve computational efficiency), we constructed trial absorption curves of the form

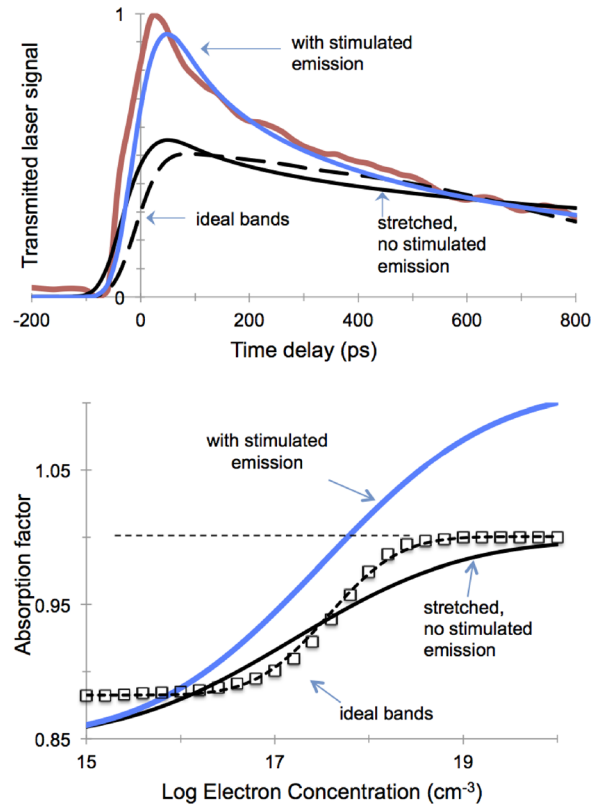


FIG. 3. Modeling x-ray induced optical transmission. Top: Calculated fits to data (top curve, from Fig. 1), assuming ideal density of states, a stretched absorption profile to simulate Urbach tails, and allowing for optical gain to simulate stimulated emission. Bottom: Absorption factor vs. conduction band electron density; the absorption factor is the relative intensity after one micron of travel. Square symbols for the “ideal bands” curve is from a standard density of state calculation; dashed line is an error function fit (see the text). The “stretched” version artificially spreads absorption over a wider electron density range, to simulate the Urbach tails in GaAs. The “with stimulated emission” curve allows the absorption to exceed unity.



$$\alpha(n) = \alpha_o + g\{1 + \text{erf}[s(\log_{10}(n) - c)]\}, \quad (4)$$

where  $\alpha_o$  is the baseline absorption,  $g$  is the gain factor initially set so  $\alpha \rightarrow 1$  for high electron densities (i.e., transparency from Pauli blocking),  $s$  is the stretching parameter that is initially unity but can be used to broaden the absorption curve, and  $c$  fixes the center of the transition. This function can reproduce the ideal bands curve without perceptible deviations (Fig. 3, bottom).

The ideal band model represented by Eq. (3) does not include the well-known Urbach tail broadening, which has been the subject of phenomenological modeling.<sup>16</sup> We emulate this broadening of the band edges by adjusting the stretching parameter in Eq. (4) to  $s = 0.5$ , which gives an only slightly improved fit (Fig. 3 top, “no stimulated emission” curve). Finally, we account for possible amplification from stimulated emission by increasing the gain factor until the maximum value of  $\alpha$  at the highest electron densities increases from unity to about 1.1, which produced a much improved fit (Fig. 3 top, “with stimulated emission” curve).

Requiring optical gain implies that stimulated emission contributes significantly to the transmitted light from x-ray pumped GaAs. Investigation of a similar system<sup>9</sup> shows a threshold electron density for an amplified spontaneous emission (ASE) of approximately  $10^{18} \text{ cm}^{-3}$ , consistent with this result. Apparently, this simple experimental configuration has in fact produced an x-ray pumped semiconductor optical amplifier: the incident laser pulse is amplified by stimulated emission from the x-ray excited conduction band electrons.

#### IV. DEPENDENCE ON LASER FLUENCE

We have so far focused on electron densities excited by x-ray absorption, which cause the enhanced transmission of the optical laser pulses via Pauli blocking. The absorption of laser photons also excites electrons and holes, however, which at sufficiently high densities increases transmission of the laser pulse itself. We now focus on a region of the data that suggests that x-ray excited electrons can perturb the laser excited electrons such that the x-rays effectively quench enhanced laser transmission. In Fig. 4, we show an expanded view of x-ray induced optical transparency data to focus on the time range where x-rays first coincide with the laser pulse. Data are given for three laser fluences, corresponding to no observable transmission without x-rays ( $20 \text{ J/m}^2$ ), an intermediate level ( $80 \text{ J/m}^2$ ), and to a high laser fluence exhibiting significant enhanced transmission ( $1100 \text{ J/m}^2$ ).

Note that at the highest fluence, there is a significant drop in the baseline laser signal near  $-70 \text{ ps}$ , long before the peak in the x-ray pulse (Gaussian width  $\sigma_\tau = 35 \text{ ps}$ ); a weaker version of this is evident in the intermediate fluence data, also displayed in Fig. 2(b). That is, while optical transmission at the x-ray fluence peak is strongly enhanced, at the leading edge of the x-ray pulse, it is suppressed. This is the opposite of x-ray induced optical transparency from Pauli blocking, where valence electrons excited by the x-ray generated photoelectrons and Auger electrons fill the bottom of the conduction band, preventing optical photons with energy near the bandgap from adding another valence electron to these already filled states.

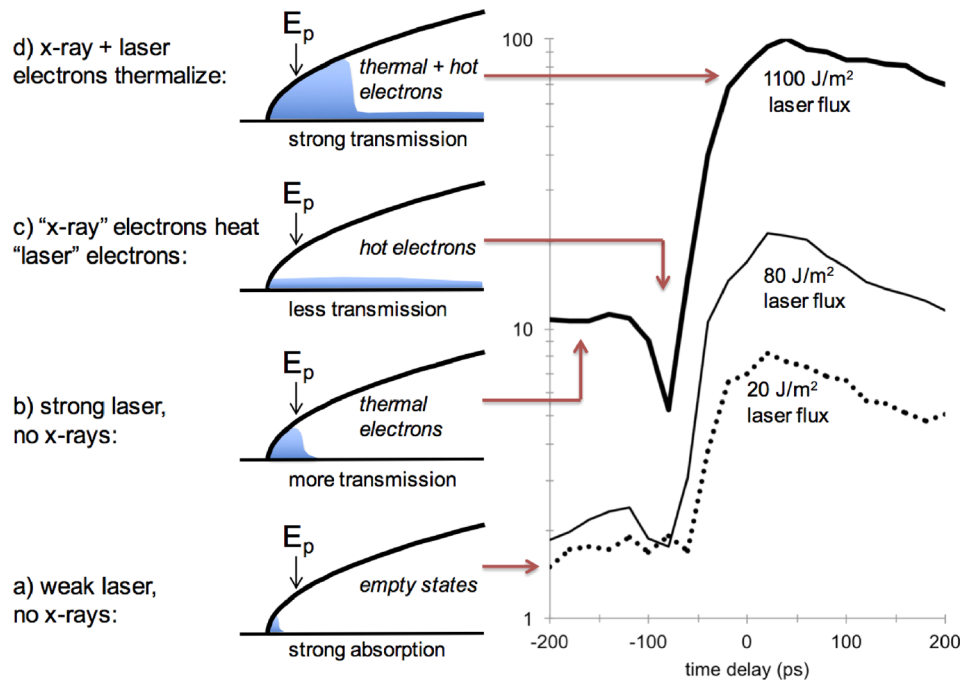


FIG. 4. X-ray induced heating of laser excited conduction electrons. (a) An ideal density of state curve is shown with mostly empty states, allowing for strong absorption.  $E_p$  denotes the energy level filled with a valence electron after absorption of a laser photon. (b) At high laser fluence, the bottom of the conduction band is filled by a thermal distribution of electrons excited by the laser pulse itself; filled states block absorption, increasing transmission. (c) Energetic x-ray induced electrons heat the laser induced electrons; the hot electron distribution unblocks the states at  $E_p$ . (d) The full x-ray fluence creates a large thermal distribution of electrons filling the bottom of the conduction band, inducing high transparency. In each case, transparency is determined by the fraction of blocked states at  $E_p$ . The data plot (right) shows transmission at both higher ( $1100 \text{ J/m}^2$ ) and lower ( $20 \text{ J/m}^2$ ) laser fluences, relative to the laser flux in the Fig. 1(b) data ( $80 \text{ J/m}^2$ ), with arbitrary units.

We propose the following explanation. The absorption of optical photons with energy just above the bandgap generates conduction electrons with minimal excess kinetic energy that can quickly thermalize to the bottom of the band. The strong absorption of these photons is reduced when densities are high enough for Pauli blocking to occur [Figs. 4(a) and 4(b)]. When an x-ray photon is absorbed, however, the resultant conduction electrons have excess energies of  $\sim 10$  eV,<sup>11</sup> and scattering with the laser-induced population of thermalized electrons will convert them into hot electrons. While various electron-electron scattering processes have characteristic lifetimes of less than 100 fs,<sup>17</sup> the evolution of hot photo-excited electrons in GaAs towards a degenerate Fermi-Dirac distribution occurs in a picosecond or so,<sup>18</sup> which is slow enough to be detectable here. This unblocks the states near the bottom of the band, allowing more absorption and quenching the enhanced optical transmission [Fig. 4(c)]. As a larger flux of x-rays is absorbed during the  $\sim 100$  ps pulse duration, a large enough fraction of the electrons thermalize to the bottom to block laser photon absorption, even as hot electrons are continuously added [Fig. 4(d)].

Quenching of laser-induced transparency is governed by the conduction electron thermalization time, roughly a picosecond or so, largely mediated by emission of LO phonons.<sup>18</sup> It may be possible to use this phenomenon to produce an ultrafast x-ray detector. The detector would be a semiconductor with a thermal distribution of degenerate conduction electrons at the bottom of the conduction band, generated by intense laser pulses or perhaps by heavy doping. A laser probe with photon energy just above the gap would have significant transmission due to Pauli blocking. X-ray absorption would heat the electrons, thus unblocking absorption. Under appropriate experimental conditions, an x-ray pump/laser probe time delay measurement would map out the time profile of the x-ray beam with a resolution of  $\sim 1$  ps. Transmission is sensitive only to the presence of filled states near the bottom of the band, and so, slower processes involving electron-hole recombination should have a negligible impact on the signal. Such a detector would be particularly useful for measuring ultrafast picosecond dynamics using  $\sim 100$  ps pulses at typical x-ray synchrotron sources.

## V. CONCLUSIONS

To summarize, we have shown that high fluence x-ray pulses absorbed by GaAs can induce not only optical transparency but also optical gain through stimulated emission. The same x-ray pulses are shown to generate surface amplified spontaneous emission in the GaAs band fluorescence spectrum. We also find that x-rays can quench enhanced laser transmission, apparently from energy exchanged between the

conduction electrons excited separately by the laser and the x-ray pulses. These results provide insight into how electronic excitations in GaAs mediate interactions between hard x-ray and optical laser pulses.

## ACKNOWLEDGMENTS

The authors acknowledge the support of Dr. Yi Xuan (Birk Nanotechnology Center, Purdue University) for the preparation of the etched GaAs specimen. This work was supported by the U.S. Department of Energy, Basic Energy Science (Grant No. DE-SC0004078) and utilized resources of the Advanced Photon Source, a U.S. Department of Energy (DOE) Office of Science User Facility operated for the DOE Office of Science by Argonne National Laboratory (Contract No. DE-AC02-06CH11357). The use of BioCARS was also supported by the National Institute of General Medical Sciences of the National Institutes of Health (Grant No. R24GM111072). The time-resolved set-up at Sector 14 was funded in part through a collaboration with Philip Anfinrud (NIH/NIDDK).

- <sup>1</sup>T. Sato, T. Togashi, K. Ogawa, T. Katayama, Y. Inubushi, K. Tono, and M. Yabashi, *Appl. Phys. Express* **8**(1), 012702 (2015).
- <sup>2</sup>S. Eckert, M. Beye, A. Pietzsch, W. Quevedo, M. Hantschmann, M. Ochmann, M. Ross, M. P. Minitti, J. J. Turner, S. P. Moeller, W. F. Schlott, G. L. Dakovski, M. Khalil, N. Huse, and A. Fohlisch, *Appl. Phys. Lett.* **106**(6), 061104 (2015).
- <sup>3</sup>C. Gahl, A. Azima, M. Beye, M. Deppe, K. Dobrich, U. Hasslinger, F. Hennies, A. Melnikov, M. Nagasono, A. Pietzsch, M. Wolf, W. Wurth, and A. Fohlisch, *Nat. Photonics* **2**(3), 165 (2008).
- <sup>4</sup>S. M. Durbin, *AIP Adv.* **2**(4), 042151 (2012).
- <sup>5</sup>S. M. Durbin, A. Landcastle, A. DiChiara, H. Wen, D. Walko, and B. Adams, *APL Photonics* **2**(8), 086102 (2017).
- <sup>6</sup>S. M. Durbin, T. Clevenger, T. Graber, and R. Henning, *Nat. Photonics* **6**, 111 (2012).
- <sup>7</sup>F. Bencivenga, R. Cucini, F. Capotondi, A. Battistoni, R. Mincigrucci, E. Giangrisostomi, A. Gessini, M. Manfredda, I. P. Nikolov, E. Pedersoli, E. Principi, C. Svetina, P. Parisse, F. Casolari, M. B. Danailov, M. Kiskinova, and C. Masciovecchio, *Nature* **520**(7546), 205 (2015).
- <sup>8</sup>T. Graber, S. Anderson, H. Brewer, Y. S. Chen, H. S. Cho, N. Dashdorj, R. W. Henning, I. Kosheleva, G. Macha, M. Meron, R. Pahl, Z. Ren, S. Ruan, F. Schotte, V. S. Rajer, P. J. Viccaro, F. Westferro, P. Anfinrud, and K. Moffat, *J. Synchrotron Radiat.* **18**, 658 (2011).
- <sup>9</sup>M. Kawase, E. Garmire, H. C. Lee, and P. D. Dapkus, *IEEE J. Quantum Electron.* **29**(8), 2306 (1993).
- <sup>10</sup>U. Strauss, W. W. Ruhle, and K. Kohler, *Appl. Phys. Lett.* **62**(1), 55 (1993).
- <sup>11</sup>B. Ziaja, R. A. London, and J. Hajdu, *J. Appl. Phys.* **97**(6), 064905 (2005).
- <sup>12</sup>N. G. Nilsson, *Appl. Phys. Lett.* **33**(7), 653 (1978).
- <sup>13</sup>J. S. Blakemore, *Solid State Electron.* **25**(11), 1067 (1982).
- <sup>14</sup>F. Stern, *Solid State Phys.* **15**, 299 (1963).
- <sup>15</sup>G. Lasher and F. Stern, *Phys. Rev. A – Gen. Phys.* **133**(2a), A553 (1964).
- <sup>16</sup>E. Y. Lin, T. S. Lay, and T. Y. Chang, *J. Appl. Phys.* **102**, 123511 (2007).
- <sup>17</sup>J. Kanasaki, H. Tanimura, and K. Tanimura, *Phys. Rev. Lett.* **113**, 237401 (2014).
- <sup>18</sup>H. Ohnishi, N. Tomita, and K. Nasu, *J. Phys. Soc. Jpn.* **84**, 043701 (2015).